Available online at www.scholarsresearchlibrary.com

Scholars Research Library

Scholars Research Library

Annals of Biological Research, 2012, 3 (11):5242-5251
(http://scholarsresearchlibrary.com/archive.html)

Annals of Biological Research
Scholars Research Library
ISSN 0976-1233
CODEN (USA): ABRNBW

A new hydrogen peroxide biosensor by using modified Carbon Paste Electrode with catalase enzyme and Mn_2O_3 Nanoparticles

Elahe Aslanpour Nikan[1], Masoud Negahdary[2*], Ehsan Nabi-abdoluosefi[1], Soheila Ghassamipour[3], Omid Motaghi[4]

[1]Department of Biology, Payame Noor University, I.R. of IRAN
[2]Young Researchers & Elite Club, Marvdasht Branch, Islamic Azad University, Marvdasht, Iran
[3]Department of Chemistry, Marvdasht Branch, Islamic Azad University, Marvdasht, Iran
[4]Pharmaceutical Research Branch, Islamic Azad University, Tehran, Iran

---

ABSTRACT

We used of Nanoscience, biology and electrochemistry in designing a new hydrogen peroxide biosensor by using modified Carbon Paste Electrode with catalase enzyme and Mn_2O_3 Nanoparticles. Cyclic voltammetry method as a general method in electrochemical studies was performed using an Autolab potentiostat. A conventional three-electrode cell was employed throughout the experiments. The produced Mn_2O_3 Nanoparticles was characterized by XRD, UV-visible, SEM and TEM analysis. The direct electrochemistry behavior of CAT / Mn_2O_3 Nps/ CPE was studied and a pair of well-defined redox peaks was observed at the CAT / Mn_2O_3 Nps/ CPE in a 0.1 mol L^{-1} phosphate buffer solution (PBS) of pH 7.0 at a scan rate of 100mVs^{-1} compared to the Mn_2O_3 Nps/ CPE. Its anodic peak potential and cathodic peak potential were located at −150mV and −200mV (vs. SCE), respectively. The formal potential (E^o) of Catalase, estimated as the midpoint of reduction and oxidation potentials, was - (175 ± 2) mV. The presented experiment has introduced a new biosensor for the sensitive determination of H_2O_2 in the solution in the range of 15-135 μM.

Keywords: biosensor, catalase, H_2O_2, Mn_2O_3 NPs, bioelectrochemistry

---

INTRODUCTION

Nanotechnology is science, engineering, and technology conducted at the nanoscale, which is about 1 to 100 nanometers [1-2]. Nanoscience and nanotechnology are the study and application of extremely small things and can be used across all the other science fields, such as chemistry, biology, physics, materials science, and engineering [3-4]. Nanotechnology is not just a new field of science and engineering, but a new way of looking at and studying. Today's scientists and engineers are finding a wide variety of ways to deliberately make materials at the nanoscale to take advantage of their enhanced properties such as higher strength, lighter weight, increased control of light spectrum, and greater chemical reactivity than their larger-scale counterparts [5-9]. Novel nanomaterials for use in bioassay applications represent a rapidly advancing field. Various nanostructures have been investigated to determine their properties and possible applications in biosensors [10-15]. These structures include nanotubes, nanofibers, nanorods, nanoparticles and thin films, of these, nanoparticles are the best studied [16]. Nanoparticles have numerous possible applications in biosensors. For example, functional nanoparticles (electronic, optical and

magnetic) bound to biological molecules (e.g. peptides, proteins, nucleic acids) have been developed for use in biosensors to detect and amplify various signals [17]. Some of the nanoparticle-based sensors include the acoustic wave biosensors, optical biosensors, magnetic and electrochemical biosensors [18-20]. Metal nanoparticles have been used to catalyze biochemical reactions and this capability can be usefully employed in biosensor design [21]. Catalysis is the most important and widely used chemical application of metal nanoparticles and has been studied extensively [22]. Transition metals show very high catalytic abilities for many organic reactions. Nanoparticles behave in the reaction medium as do conventional homogeneous catalysts, but can be easily recovered after the reaction [23-25]. Metal nanoparticles can be used as an electrochemical label. Most biological molecules can be labeled with metal nanoparticles without compromising their biological activities [26-27]. Affinity assays can then be performed by monitoring the electrochemical signal of these metal nanoparticles. Catalase is one of the most potent catalysts known. The reactions it catalyses are crucial to life [28]. Catalase does catalysis conversion of Hydrogen Peroxide, a powerful and potentially harmful oxidizing agent, to water and molecular oxygen. Catalase also uses Hydrogen Peroxide to oxidise toxins including Phenols, Formic Acid, Formaldehyde and Alcohols [29-30]. Catalase is a heme containing redox enzyme. It is found in high concentrations in a compartment in cells called the peroxisome [31]. H_2O_2 is a powerful oxidizing agent and is potentially damaging to cells. By preventing excessive H_2O_2 build up Catalase allows important cellular processes which produce H_2O_2 as a byproduct to take place safely. The Fe (III)/Fe (II) redox state could be found in Catalase by electron exchange [32-33].The Three-dimensional structure of Catalase was shown in figure 1[34].

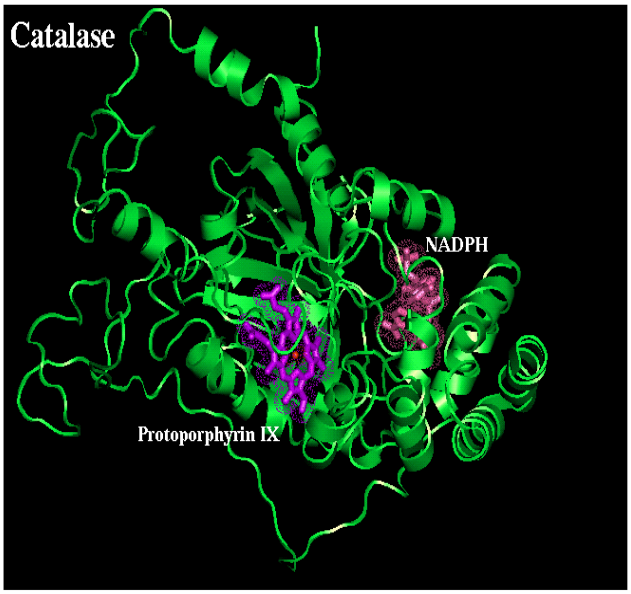

Figure 1. Three-dimensional structure of CAT.

Here we used of Nanoscience (Mn_2O_3 NPs), biology (catalase enzyme) and electrochemical method (conventional three-electrode cell) for designing a new biosensor for H_2O_2 detection.

MATERIALS AND METHODS

2.1. Materials

Catalase from bovine liver (40-45 units/ mg) and Mn (III) acetylacetonate purchased from Sigma-Aldrich. Other Reagents such as H_2O_2 purchased from Merck. The supporting electrolyte used for all experiments was 0.1 M pH 7 phosphate buffer solution (PBS), which prepared by using 0.1 M Na_2HPO_4 and NaH_2PO_4 solutions. All the reagents used were of analytical grade and all aqueous solutions were prepared using doubly distilled water generated by a Barnstead water system.

2.2. Apparatus

Cyclic voltammetry method were performed using an Autolab potentiostat PGSTAT 302 (Eco Chemie, Utrecht, The Netherlands) driven by the General purpose Electrochemical systems data processing software (GPES, software

version 4.9, Eco Chemie). A conventional three-electrode cell was employed throughout the experiments, with bare or Mn_2O_3 Nps modified CPE (3.0mm diameter) as a working electrode, a saturated calomel electrode (SCE) as a reference electrode, and a platinum electrode as a counter electrode; Reference and counter electrodes were purchased from Azar electrode Co (IR. Iran). The phase characterization of Mn_2O_3 Nps was performed by means of XRD using a D/Max-RA diffractometer with CuKα radiation. The absorbance properties of prepared nanoparticles were measured and recorded by using a TU-1901 double-beam UV-visible spectrophotometer. The morphologies and particle sizes of the samples were characterized by JEM-200CX TEM working at 200 kV, and SEM image was obtained with a ZIESS EM 902A SEM.

2.3. Preparation of Mn_2O_3 Nps

Mn_2O_3 Nps were synthesized by heating Mn (III) acetylacetonate (1 mmol, 0.35 g) in 20 mL acetone or ethanol in a Teflon-lined Parr acid-digestion bomb at 200°C for a minimum of 72 hours. The dark product solution was dispersed in chloroform and centrifuged for 10 minutes. The black precipitate was isolated and dried at Room Temperature under vacuum for 12 hours, followed by calcination at 500°C for 4 hours. The product was characterized by XRD, UV-visible, SEM and TEM analysis.

2.4. Preparation of unmodified CPE and modified CPE with Mn_2O_3 Nps

Unmodified CPE was prepared by mixing 65% graphite powder and 35% paraffin wax. Paraffin wax was heated till melting and then, mixed very well with graphite powder to produce a homogeneous paste. The resulted paste was then packed into the end of an insulin syringe (i.d.: 3.0mm). External electrical contact was established by forcing a copper wire down the syringe. CPE modified with Mn_2O_3 Nanoparticles was prepared by mixing 60% graphite powder and 30% paraffin wax with and 10% Mn_2O_3 Nps. The surface of the electrode was polished with a piece of weighting paper and then rinsed with distilled water thoroughly.

2.5. Preparation of CAT- Mn_2O_3 Nps modified CPE

The modified CPE electrode that produced in previous section was used for production of CAT-Mn_2O_3 Nps modified CPE. In this section, the CAT was immobilized by dropping 5 µl of 10 mg/ml of the protein solution onto the Mn_2O_3 Nps modified CPE and dried for about 30 min at room temperature. The electrode was then gently washed with de-ionized double distilled water and put at 4 ºC when not in use.

RESULTS AND DISCUSSION

3.1. UV-visible spectroscopy of Mn_2O_3 Nps

UV-visible spectroscopy is one of the most widely used techniques for structural characterization of metal nanoparticles [35]. These nanoparticles exhibit a strong UV-vis absorption band that is not present in the spectrum of the bulk state [36]. The UV-VIS spectral range is approximately 190 to 900 nm, as defined by the working range of typical commercial UV-VIS spectrophotometers. According to Fig. 2(a&b), you can see that in nano size state, material show a different UV-VIS spectra ratio to bulk state. As it is clear, intensity units was increased and improved in Mn_2O_3 Nps (Fig. 2(b)) due to the quantum confinement of the excitons present in the sample compare with bulk Mn_2O_3 particles (Fig. 2(a)). This phenomenon indicates that these Nps show the quantum size effect [37].

3.2. X-Ray diffraction of Mn_2O_3 Nps

The XRD pattern Fig. 3 for Mn_2O_3 Nps, the diffraction peaks are absorbed at 2θ values. The prominent peaks have been utilized to estimate the grain size of sample with the help of Scherrer equation [38] $D = K\lambda/(\beta \cos \theta)$ where K is constant(0.9), λ is the wavelength(λ = 1.5418 A°) (Cu Kα), β is the full width at the half-maximum of the line and θ is the diffraction angle. The grain size estimated using the relative intensity peak for Mn_2O_3 Nps was found to be 70 nm and increase in sharpness of XRD peaks indicates that particles are in crystalline nature. All peaks in Fig. 3 related to Mn_2O_3 Nps and matched to Joint Committee for Powder Diffraction Studies (JCPDS).

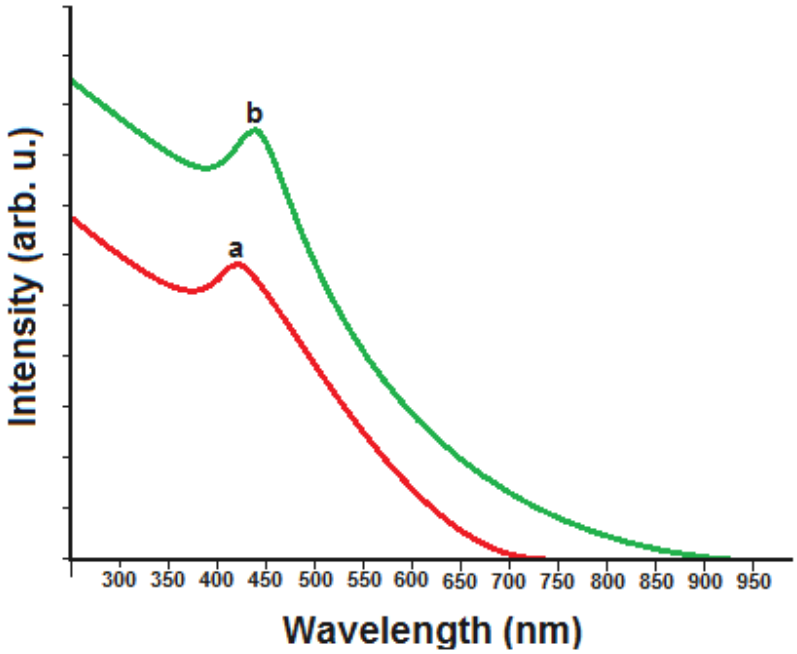

Figure 2. UV-visible spectroscopy for (a) bulk Mn_2O_3 particles; (b) Mn_2O_3 Nps.

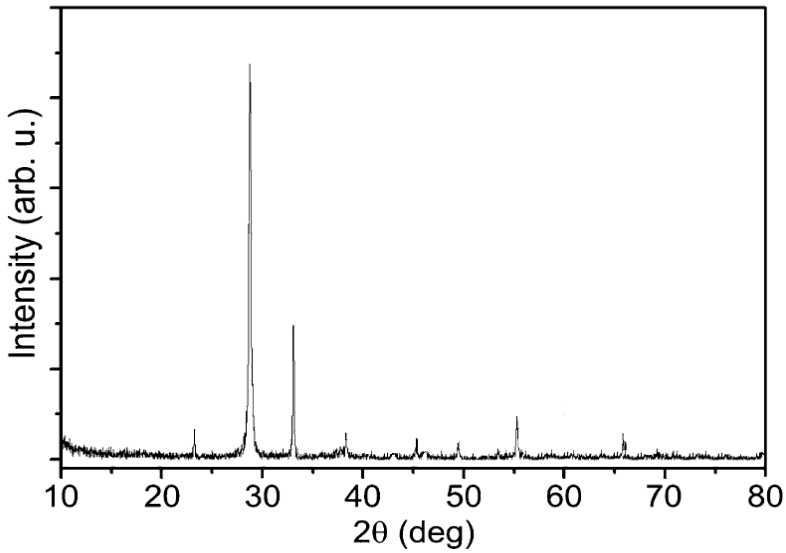

Figure 3. XRD pattern for Mn_2O_3 Nps.

3.3. Microscopic characterization of Mn_2O_3 Nps

As it is well known, the properties of a broad range of materials and the performance of a large variety of devices depend strongly on their surface characteristics. Morphology of the Mn_2O_3 Nps was investigated by using of TEM and SEM. Parts (a) and (b) of Fig. 4 show the typical TEM and SEM images of the sample respectively. The SEM image was captured in 1 µm scale bar and the TEM image was captured in 100 nm scale bar. The average diameter of the Synthesized Mn_2O_3 Nps was about 70 nm, and had a very narrow particle distribution.

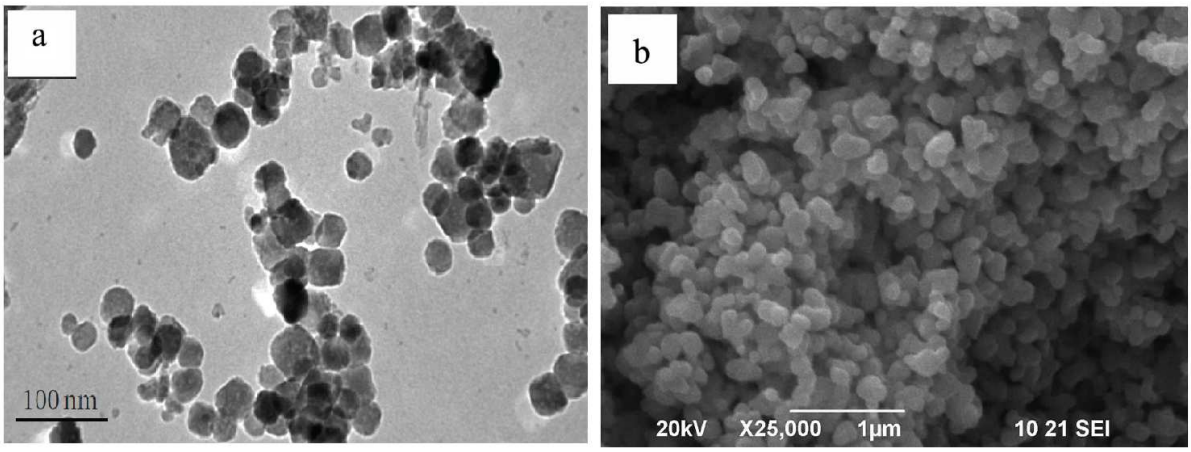

Figure 4. (a) TEM image and (b) SEM image, of Mn_2O_3 NPs.

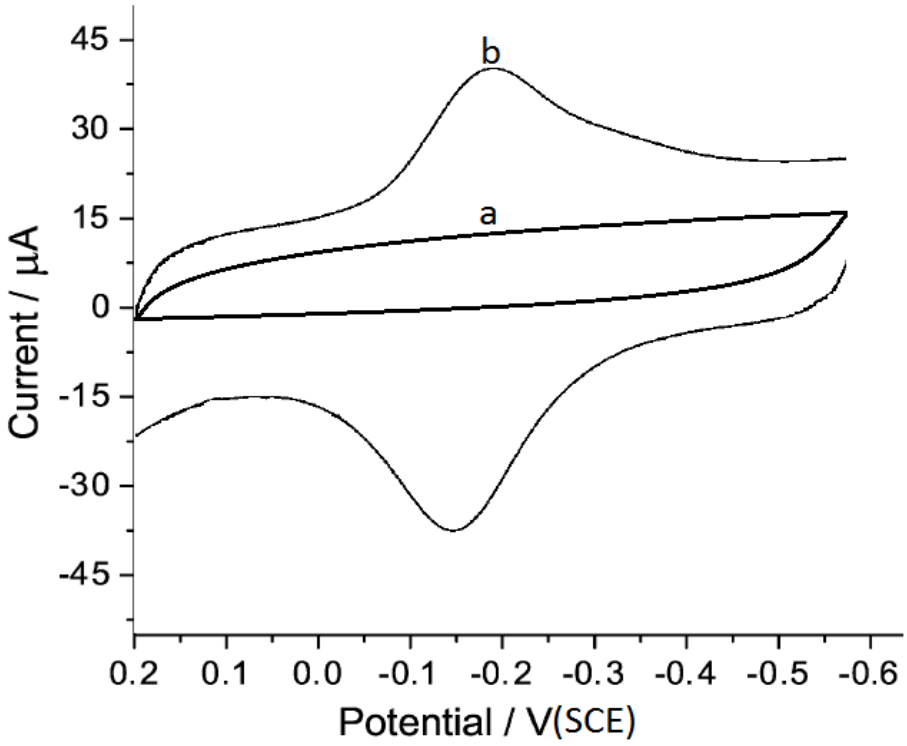

Figure 5. Cyclic voltammograms, using (a) the Mn_2O_3 Nps/ CPE in 0.1 M phosphate buffer and (b) CAT / Mn_2O_3 Nps/ CPE in 0.1 M phosphate buffer solution (scan rate: 100 mV/s).

3.4. Direct voltammetric behavior of the CAT/ Mn_2O_3 NPs/CPE electrode

The direct electrochemistry behavior of CAT / Mn_2O_3 Nps/ CPE was studied as shown in Fig. 5. It can be seen in cyclic voltammograms (Fig. 5 (b)) that a pair of well-defined redox peaks was observed at the CAT / Mn_2O_3 Nps/ CPE in a 0.1 mol L^{-1} phosphate buffer solution (PBS) of pH 7.0 at a scan rate of 100mVs^{-1} compared to the Mn_2O_3 Nps/ CPE (Fig. 5 (a)). Its anodic peak potential and cathodic peak potential were located at −150mV and −200mV (vs. SCE), respectively. Obviously, these peaks were attributed to the redox reaction of the electroactive probe of Catalase. CAT / CPE also showed the response of Catalase, but the response was much smaller than that of CAT / Mn_2O_3 Nps/ CPE (not shown). Thus, the adsorption of Catalase and Mn_2O_3 nanoparticles on electrode surface played an important role in facilitating the electron exchange between the electroactive center of Catalase and CPE.

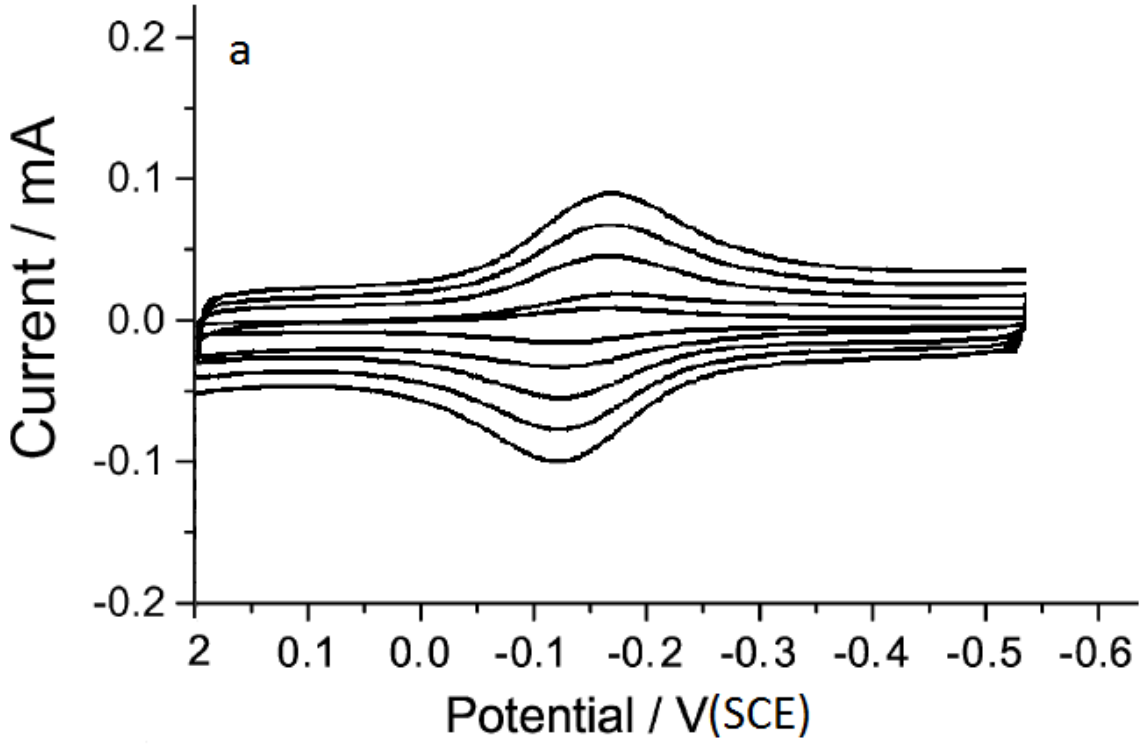
a
Current / mA
0.2
0.1
0.0
-0.1
-0.2
2
0.1
0.0
-0.1
-0.2
-0.3
-0.4
-0.5
-0.6
Potential / V(SCE)

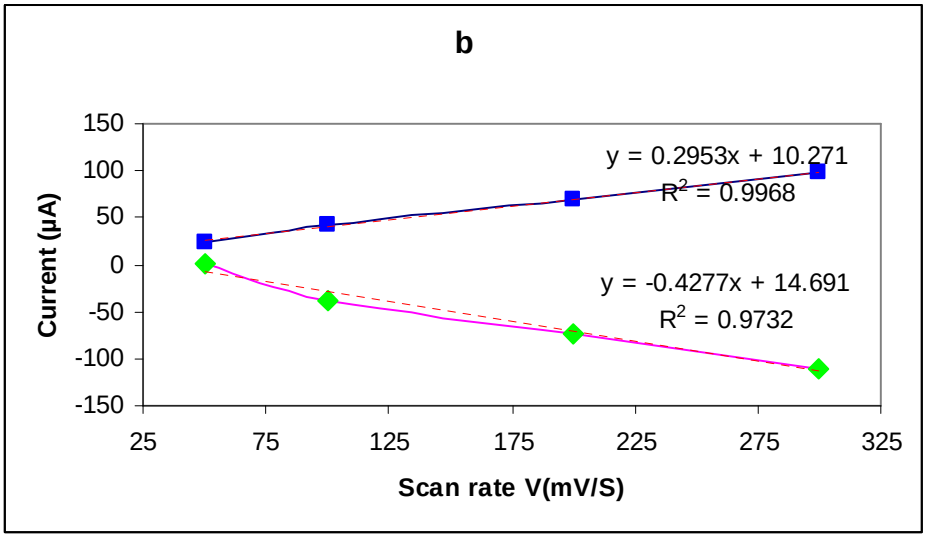
b
Current (µA)
150
100
50
0
-50
-100
-150
25
75
125
175
225
275
325
Scan rate V(mV/S)
y = 0.2953x + 10.271
R2 = 0.9968
y = -0.4277x + 14.691
R2 = 0.9732

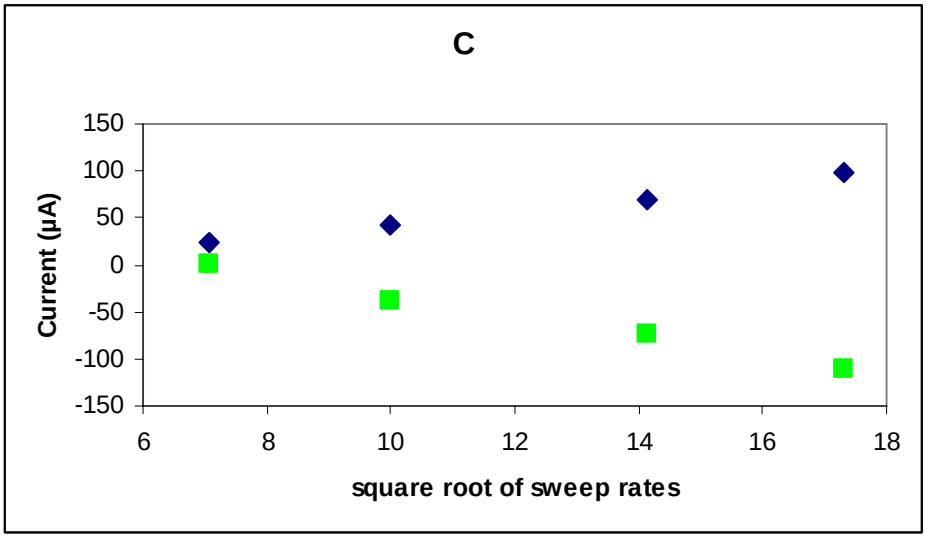

Figure 6. (a) CVs of CAT / Mn_2O_3 Nps/ CPE in PBS 0.1M at various scan rates, from inner to outer; 50, 100, 200, and 300 mV s^{-1}, the relationship between the peak currents (ipa, ipc) vs., (b) the sweep rates and (c) the square root of sweep rates. Blue lines are reduction peaks and green lines are oxidative peaks.

The formal potential (E^o) of Catalase, estimated as the midpoint of reduction and oxidation potentials, was - (175 ± 2) mV.

Fig. 6(a) shows the cyclic voltammograms of the CAT / Mn_2O_3 Nps/ CPE in 0.1 mol L^{-1} phosphate buffer solution of pH 7.0 at different scan rates (50, 100, 200, and 300 mV s^{-1}). The peak currents increased and the cathodic and anodic peak potentials exhibited a small shift along with the increase of scan rate. On the grounds that the surface-to-volume ratio increases with the size decrease and because of the fact that the catalase enzyme size is comparable with the nanometer-scale building blocks, these nanoparticles displayed a great effect on the electron exchange assistance between CAT and carbon paste electrode. For further investigate the CAT characteristics at the CAT / Mn_2O_3 Nps/ CPE, the effect of scan rates on the CAT voltammetric behavior was studied in detail. The baseline subtraction procedure for the cyclic voltammograms was obtained in accordance with the method reported by Bard and Faulkner [39]. The scan rate (ν) and the square root scan rate ($\nu^{1/2}$) dependence of the heights and potentials of the peaks are plotted in Fig. 6b and c. It can be seen that the redox peak currents increased linearly with the scan rate, the correlation coefficient was 0.9968 (ipc = 0.2953ν +10.271) and 0.9732 (ipa = -0.4277ν +14.691), respectively. This phenomenon suggested that the redox process was an adsorption-controlled and the immobilized alcohol dehydrogenase was stable. It can be seen that the redox peak currents increased more linearly with the ν in comparison to that of $\nu^{1/2}$.

All these results indicated that the CAT immobilized into Mn_2O_3 Nps / CPE underwent a surface controlled and quasi-reversible electrochemical reaction process. When the peak-to-peak separation (ΔE) was larger than 200 mV, the apparent heterogeneous electron transfer rate constants (k_s) would be easily calculated with the help of Laviron's consistent with the reported potential values for redox state in the CAT. These results suggested that direct electron transfer of the CAT molecules entrapped in Mn_2O_3 Nps/ CPE was enhanced. However, there is clearly a systematic deviation from linearity in this data, i.e. low scan rates are always on one side of the line and the high scan rate points are on the other. The anodic and cathodic peak potentials are linearly dependent on the logarithm of the scan rates (ν) when ν > 1.0 V s^{-1}, which was in agreement with the Laviron theory, with slopes of -2.3RT/αnF and 2.3RT/ (1 -α) nF for the cathodic and the anodic peak, respectively [40]. So, the charge-transfer coefficient (α) was estimated equal to 0.55. (Given $0.3 < \alpha < 0.7$ in general). Furthermore, the heterogeneous electron transfer rate constant (ks) was estimated according to the following equation [41]:

$$[\log ks = \alpha \log(1-\alpha) + (1-\alpha)\log\alpha - \log\frac{RT}{nF\nu} - \frac{\alpha(1-\alpha)nF\Delta EP}{2.3\,RT}] \quad (1)$$

Here, n is the number of transferred electrons at the rate of determining reaction and R, T and F symbols having their conventional meanings. ΔE_p is the peak potential separation. The ΔE_p was equal to 21, 79.5, 143.75 and 208 mV at 50, 100, 200 and 300 mV s^{-1}, respectively, giving an average heterogeneous transfer rate constant (ks) value of 1.86 s^{-1}.

3.5. Application of CAT - Mn_2O_3 nanoparticles modified carbon paste electrode for H_2O_2 concentration determination

The cyclic voltammograms of the CAT - Mn_2O_3 nanoparticles modified carbon paste electrode in PBS, at pH 7.0, containing different concentrations of H_2O_2 shown in Figure 7a. Upon the addition of H_2O_2 to the electrochemical cell, the reduction peak current of the immobilized CAT increased, indicating a typical electro-catalytic behavior to the reduction of H_2O_2. The electro-catalytic process could be expressed as follows.

CAT-Fe (III) + e^- + H^+ ↔ CAT -Fe (II) H^+ *at the electrode surface* (2)

H_2O_2 + CAT-Fe (II) H^+ → CAT-Fe (III) + H^+ + H_2O_2 *in the solution* (3)

The calibration curve (Figure 7b) shows the linear dependence of the cathodic peak current on the H_2O_2 concentration in the range of 15-135 μM. The relative standard deviation was 3.3% for 4 successive determinations at 25 μM and the detection limit was 12 μM. The recent experiment has introduced a new biosensor for the sensitive determination of H_2O_2 in the solution.

Decreasing the redox potential and the use of wide pH range are the main purposes during the designing process of a sensor. So, to fulfill the above requirements, CAT -modified electrodes are being used, by different workers, for H_2O_2 determination. The present work, Mn_2O_3 oxide nanoparticles became immobilized after its deposition on the surface of carbon paste electrode, without using any other immobilizer. Therefore, it is shown that the carbon paste electrode does not need any immobilizer of other materials for helping it in attaching to the surface of electrode. In comparison to the previous works, our work shows the facilitated electron-transfer of CAT to the surface of electrode and vice versa, and the preparation of the modified electrode is easier and faster than that stated in these previous studies. Moreover, graphite powder and paraffin for produce of carbon paste electrode is much cheaper and less rare than the other electrodes.

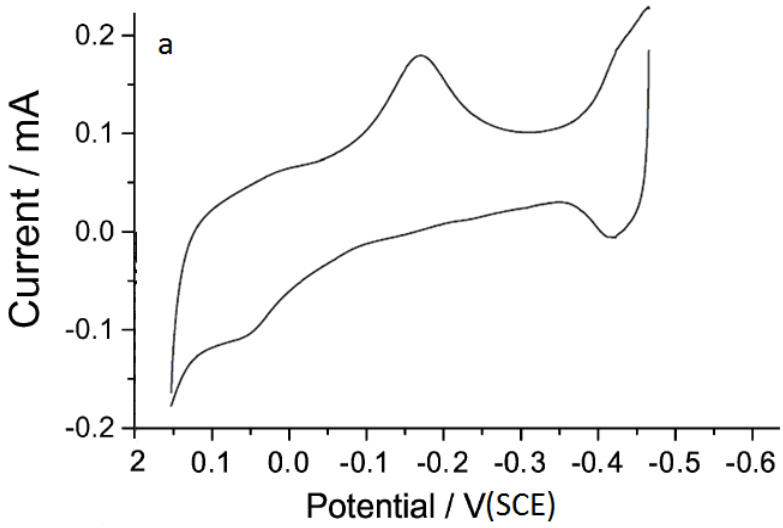

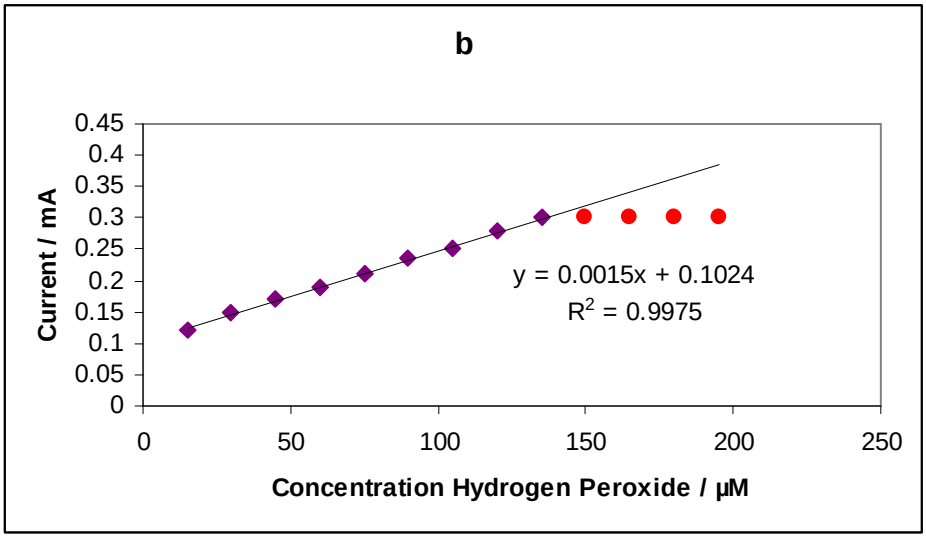

Figure 7. a) Cyclic voltammograms obtained at an CAT - Mn_2O_3 nanoparticles modified carbon paste electrode in 0.1 M PBS (pH 7.0) for 25.0µM concentration of H_2O_2 and b) the relationship between cathodic peak current of CAT and different concentrations of H_2O_2 (scan rate: 100 mVs^{-1}).

CONCLUSION

In presented work Application of CAT - Mn_2O_3 nanoparticles modified carbon paste electrode for H_2O_2 concentration determination was investigated. Nanotechnology is revolutionizing the development of biosensors. Nanomaterials and nanofabrication technologies are increasingly being used to design novel biosensors. The linear dependence of the cathodic peak current on the H_2O_2 concentration was in the range of 15-135 µM. The relative standard deviation was 3.3% for 4 successive determinations at 25 µM and the detection limit was 12 µM. The recent experiment has introduced a new biosensor for the sensitive determination of H_2O_2 in the solution.

REFERENCES

[1] Kress-Rogers, E. *Handbook of Biosensors and Electronic Noses*; CRC Press Inc.: New York, **1997**.
[2] Wise, D.L. *Bioinstrumentation and Biosensors*; Marcel Dekker: New York, **1991**.
[3] Turner, A.P.F.; Karube, I.; Wilson, G.S. *Biosensors Fundamentals and Applications*; Oxford Univeristy Press: Oxford, **1987**.
[4] J.J. Ramsden, What is nanotechnology? *Nanotechnology Perceptions*, **2005**, 1, 3–17.
[5] F. Allhoff, P. Lin, J. Moor and J. Weckert (eds), Nanoethics: *The Ethical and Societal Implications of Nanotechnology*. Chichester: Wiley, **2007**.
[6] J. Altmann, *A review of the potential military market for nanotechnology and current research activity*. Military Nanotechnology. London: Routledge, **2006**.
[7] Rosi N L, Mirkin C A. *Chem. Rev*. **2005**, 105, 2, 1547.
[8] Matsudai M, and Hunt G. *Nippon Koshu Eisei Zasshi*, **2005**, 52, 11, 923.
[9] Baibarac M, Gomez-Romero P. *J. Nanosci. Nanotechnol*. **2006**; 6, 2, 289.
[10] Masoud Negahdary, Seyedeh Anousheh Sadeghi, Masomeh Hamrahi-michak, Saeed Rezaei-Zarchi, Fatemeh Salahi, Narjes Mohammadi, Elahe Azargoon and Aida Sayad, *Int. J. Electrochem.* Sci., **2012**, 7, 6059 – 6069.
[11] Masoud Negahdary, Asadollah Asadi, Shokoufeh Mehrtashfar, Mojtaba Imandar, Hajar Akbari-dastjerdi1, Fatemeh Salahi, Azar Jamaleddini and Marziyeh Ajdary, *Int. J. Electrochem. Sci*., **2012**, 7, 5185 – 5194.
[12] Sedigheh Banapour, Manouchehr Mazdapour, Zahra Dinpazhooh, Fatemeh Salahi, Mahdi Torkamani Noughabi, Masoud Negahdary, Aram Asrari, Faezeh Ghanami, *Advanced Studies in Biology*, **2012**, 4, 5, 231 – 243.
[13] Masoud Negahdary, Somaye Rad, Mahdi Torkamani Noughabi, Ali Sarzaeem, Saeid Pasban Noughabi, Fazlollah Mirzaeinasab, Manouchehr Mazdapour and Somaye Amraeifard, *Advanced Studies in Biology*, **2012**, 4, 3, 103 – 118.

[14] Masoud Negahdary, Mahdi Torkamani Noughabi, Esmaeil Rezaei, Manouchehr Mazdapour, Alireza Farasat, Tahereh Arabnezhad-khanooki, Batool Yousefi-telori, Fazlollah Mirzaeinasab-nasab, *Advances in Environmental Biology*, **2012**, 6, 3, 1095-1103.
[15] Masoud Negahdary, Gholam reza Mazaheri, Somyyeh Rad, Mohammadreza Hadi, Roya Malekzadeh, Mohammad Mahdi Saadatmand, Saeed Rezaei-Zarchi, Fariba Pishbin, and Mojdeh Khosravian-hemami. *International journal of analytical chemistry*, **2012**, Article ID 375831, 7 pagesdoi:10.1155/2012/375831.
[16] Benhar, I., Eshkenazi I., Neufeld, T., Opatowsky, J., Shaky, S., and Rishpon, *J. Talanta*, **2001**, 55, 899–907.
[17] Bertozzi, C.R., and Kiessling, L.L, Chemical Glycobiology. *Science*, **2001**, 291, 2357–2364.
[18] Brandt, O., and Hoheisel, *J.DTrends Biotechnol*, **2004**, 22, 617–622.
[19] Cardullo, F., Diederich, F., Echegoyen, L., Habicher, T., Jayaraman, N., Leblanc, R.M., Stoddart, J.F., and Wang, S. Langmuir, **1998**, 14, 1955–1959.
[20] Emanuel, P.A., Dang, J., Gebhardt, J.S., Aldrich, J., Garber, E.A.E., Kulaga, H., Stopa, P, Valdes, J.J., and Dion-Schultz, A, *Biosens. Bioelectron*, **2000**, 14, 751–759.
[21] J. B. Raoof, Ojani, and A. Kiani, *J. Electroanal. Chem*, **2001**, 515, 45
[7] D. R. Shankaran, K. Limura, T. Kato, *Sens, Actuators, B, Chem*, **2003**, 94, 73.
[22] J. W Mo, B. Ogoreve. *Anal Chem*, **2001**, 73, 1196.
[23] R. Thanavelan, G. Manikandan, G. Ramalingam, V. Thanikachalam, *Der Chemica Sinica*, **2011**, 2, 4, 90-98.
[24] H P Klug, L E Alexander, Wiley, New York, **1954**.
[25] Haiming Fan, Lintao Yang, *Nanotechnology*, **2004**, 15, 37
[26] X. R. Ye, C. Daraio, C. Wang, J. B. Talbot, *Jin Journal of Nanoscience and Nanotechnology*, **2006**, 6 ,852.
[27] E.A. Meulenkamp, *J. Phys. Chem*, **1998**, 102, 7764.
[28] Gemeiner, P., Docolomansky, P., Vikartovska, A., and Stefuca, V, *Biotechnol. Appl. Biochem*. **1998**, 28, 155–161.
[29] Majumdar, A., and Thundat, T, *Anal. Chem*, **2001**, 73, 1567–1571.
[30] D.Nagarjuna Reddy, K.Vasudeva Reddy, T. Sreenivasulu Reddy and K. Hussain Reddy, *Der Chemica Sinica*, **2011**, 2 , 4, 123-132.
[31] Subrahmanyam, S., Piletsky, S.A., and Turner, A.P.F, *Anal. Chem*, **2002**, 74, 3942–3952.
[32] Sachin. V. Bangale, S. M. Khetre and S. R. Bamane, *Der Chemica Sinica*, **2011**, 2, 4, 303-311.
[33] Tien, H.T.; Wurster, S.H.; Ottova, A.L. *Bioelectrochem Bioenerg*, **1997**, 42, 77–94.
[34] K.J. Huang, .D.J. Niu, X. Liu, Z.W. Wu, Y. Fan, Y.F. Chang, Y.Y. Wu, *Electrochim. Acta*, **2011**, 56, 2947.
[35]Haiming Fan, Lintao Yang, *Nanotechnology*., **2004**, 15, 37.
[36]Jeremy Ramsden, *Essentials of Nanotechnology*, Ventus Publishing ApS. **2009**.
[37]H. Ju, S. Liu, B.Ge, F. Lisdat, F.W. Scheller, *Electroanalysis*, **2002**,14, 141.
[38]H. Fan, L. Yang, W. Hua et al., *Nanotechnology*, **2004**,15, 37.
[39]A.J. Bard, L.R. Faulkner, *Electrochemical Methods*, second. ed., Fundamentals and Applications, Wiley, NY, **2001**, 241.
[40] E. Laviron. *Journal of Electroanalytical Chemistry*., **1979**, 101, 1, 19-28.
[41] E. Laviron. *Journal of Electroanalytical Chemistry*., **1979**, 100, 263-270.